Science of the Total Environment 866 (2023) 161397

Contents lists available at ScienceDirect

Science of the Total Environment

journal homepage: www.elsevier.com/locate/scitotenv

Ageing characteristics and microplastic release behavior from rainwater facilities under ROS oxidation

Chao Liu [a,b], Xiaoran Zhang [a,b,*], Junfeng Liu [c], Zhifei Li [d], Ziyang Zhang [b], Yongwei Gong [a], Xiaojuan Bai [a,b], Chaohong Tan [a,b], Haiyan Li [b], Junqi Li [a], Yuansheng Hu [e]

[a] Key Laboratory of Urban Stormwater System and Water Environment, Ministry of Education, Beijing University of Civil Engineering and Architecture, Beijing 102616, China
[b] Beijing Engineering Research Center of Sustainable Urban Sewage System Construction and Risk Control, Beijing University of Civil Engineering and Architecture, Beijing 100044, China
[c] Department of Water Conservancy and Civil Engineering, Beijing Vocational College of Agriculture, Beijing 102442, China
[d] Beijing General Municipal Engineering Design & Research Institute Co., Ltd, Beijing 100044, China
[e] Department of Civil Engineering and Construction, Faculty of Engineering and Design, Atlantic Technological University Sligo, Ash Lane, Sligo F91YW50, Ireland

HIGHLIGHTS

- High microplastic release from rainwater facilities during ROS-induced ageing.
- Release amount ranged from 158 to 6617 items/g, following PP > HDPE > PVC facility.
- Microplastic size ranged from 2 to 1362 μm, dominated by 10–30 μm fraction (62.7 %).
- Increased linearly with ageing time and exponentially with decreasing particle size.
- The release of microplastic depended on the composed materials and ageing time.

GRAPHICAL ABSTRACT

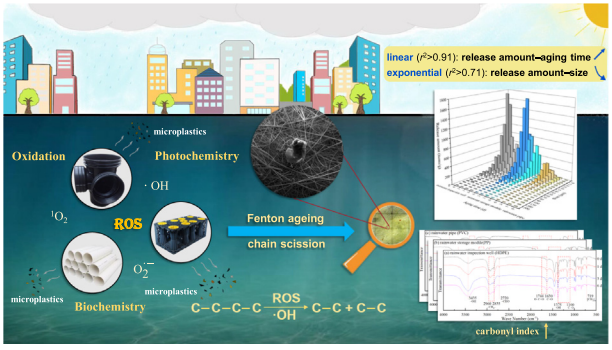

ARTICLE INFO

Editor: Kevin V. Thomas

Keywords:
Microplastic
Rainwater facility
Release
Fenton reagent
ROS
Ageing

ABSTRACT

Reactive oxygen species (ROS) are ubiquitous in the natural environment that are generated by chemical or biochemical processes. Plastic rainwater facilities, as an important part of modern rainwater systems, are inevitably deteriorated by ROS. As a consequence, microplastics will be released. However, information on how ROS affect the ageing characteristics of plastic rainwater facilities and the subsequent microplastic release behavior is still insufficient. To address this knowledge gap, Fenton reagents were used to simulate the reactive oxygen species (ROS) induced ageing process of three typical plastic rainwater components (rainwater pipe, made of polyvinyl chloride; modular storage tank, made of polypropylene; inspection well, made of high-density polyethylene) and the subsequent microplastic release behavior. After 6 days of Fenton ageing, an increase in sharpness, holes, and fractures on the rainwater facilities' surface was observed by scanning electron microscope (SEM). The functional group changes on the rainwater facilities' surface were analyzed by Fourier transform infrared spectrometer (FTIR) and two-dimensional correlation spectroscopy (2D-COS) and compared with the results of X-ray photoelectron spectroscopy (XPS). During the ageing process, oxygen-containing functional groups were generated and the carbon chains were broken, which promoted peeling and the release of microplastics. The amount of released microplastics (ranging from 158 to 6617 items/g facility) varied with the type of rainwater facilities, and the order was modular storage tank > inspection well > rainwater pipe. The release amount increased with ageing time, and a significant linear relationship was observed (r^2 > 0.91). The particle size of the released microplastics ranged from 2 to 1362 μm, among which 10–30 μm particles

* Corresponding author at: Key Laboratory of Urban Stormwater System and Water Environment, Ministry of Education, Beijing University of Civil Engineering and Architecture, Beijing 102616, China.
E-mail address: zhangxiaoran@bucea.edu.cn (X. Zhang).

http://dx.doi.org/10.1016/j.scitotenv.2023.161397
Received 18 September 2022; Received in revised form 30 November 2022; Accepted 1 January 2023
Available online 4 January 2023

accounted for the largest proportion (62.7 %). The release amount increased exponentially with decreasing particle size ($r^2 > 0.71$). This study indicates that large amounts of microplastics could be released from plastic rainwater components during ROS-induced ageing.

1. Introduction

Plastic products are inexpensive, stable, and versatile. According to statistics, 300 million tons of plastics are produced globally every year, of which 260 million tons are discarded, and nearly 20 % of them are ecologically harmful (Toensmeier, 2020). Plastic products in the environment will be degraded by light, hydraulic scouring, bacteria, free radicals, and other factors, forming microplastics (MPs, particle size<5 mm) and then released into the environment. Microplastic pollution first attracted people's attention in marine environments and was subsequently found in rivers, lakes, sediments, soils, wetlands, road dust, etc. (Hu et al., 2022). Many studies have confirmed that microplastics can not only be bio-concentrated but also adsorb environmental pollutants, which are potentially harmful to organisms in the ecological environment (Eom et al., 2021).

With the development of modern cities, the requirement for urban flood prevention and drainage capacity is increasing, and plastic rainwater facilities are widely installed, such as drainage pipes, inspection wells, pollutants intercepting baskets, downspouts, rainwater storage modules, and initial discarded flow filtration devices, etc. (Qin et al., 2021). They are composed of a variety of plastics, including polystyrene (PS), polyvinyl chloride (PVC), polyethylene (PE), polycarbonate (PC), polypropylene (PP), and Acrylonitrile butadiene Styrene copolymers (ABS), etc. After installation, rainwater facilities inevitably undergo various physical, chemical, and biological ageing processes (Miranda et al., 2021), which lead to the release of microplastics during their service life. In our previous study, significant amounts of microplastic particles (160 to 1905 items/g) were released from rainwater facilities after UV ageing and hydraulic scouring (Zhang et al., 2022).

Reactive oxygen species (ROS) are intermediates formed during the sequential single-electron reduction of oxygen and are widely present. In the natural environment, ROS could be formed from various processes such as photochemical and biological processes (Gali et al., 2020). Morris et al. (2022) reviewed ROS in the ocean and their environmental impacts, noting that ROS in surface seawater are mainly generated by photochemical processes of dissolved organic matter or released from the stress reactions of marine organisms; in addition, ROS are also generated by abiotic non-photochemical processes, such as ROS in hydrothermal vents. Murphy et al. (2016) showed that S^{2-} was oxidized by O_2 in the presence of hydrous iron oxide to produce $O^{\bullet-}_2$ and H_2O_2. Han et al. (2022a) researched soil organic matter-mediated microbial iron reduction and hydroxyl radical production, and indicated that hydroxyl radicals are produced during both bacterial iron reduction and oxidation of soil organic matter. Song et al. (2022) investigated the effects of the nature of dissolved organic matter on ROS photo-production in lake flood and drought periods, indicating that steady-state concentrations of ROS could significantly reduce the half-life of ethephon in Poyang Lake during flood.

The rainwater facilities under working conditions, exposed to water and soil environment, are inevitably affected by the ageing of ROS. Jiang et al. (2021) studied the reaction process of C—C bond oxidation by hydroxyl radicals in PE through quantum chemical calculations, and pointed out that hydroxyl radicals were able to extract hydrogen from PE fragments and initiate the subsequent cleavage reaction. Duan et al. (2022) demonstrated that ROS not only caused the structural change of plastics and the formation of microplastics, but also affects their migration and distribution in the aqueous environment. Zhu et al. (2020) found that UV–visible light can induce the production of ROS such as ·OH, $O^{\cdot}_2$, and $^1O_2$. Shi et al. (2021) investigated the degradation pathway of PC MPs and pointed out that the photo-ageing of PC MPs was mainly caused by the generated ROS. Liu et al. (2022) indicated that among all the generated ROS, ·OH was a key species for accelerating the degradation of plastic. In addition, Han et al. (2022b) noted that ROS would be produced during the oxidation of structural ferrous iron in the soil environment. Bai et al. (2022) investigated the ageing effect of pyrite-induced ROS on PS microplastics under light conditions, noting that ·OH radicals play the strongest role as the most widespread sulfide metal mineral on the surface accelerating the ageing behavior of microplastics in the environment and increasing the environmental risk. Usually, rainwater facilities are placed in a complex environment, where they may expose to solar irradiation and in long-term contact with water and soil (Nielsen et al., 2008; Li et al., 2021). Therefore, ROS oxidation could be an important process that causes the ageing of plastic rainwater facilities and the subsequent release of microplastics. However, the effects of ROS on plastic rainwater facilities remain poorly understood due to the relatively low concentrations of oxidants in the aquatic environment, resulting in a long time for the natural ageing process.

As an advanced oxidation technology, the Fenton reaction is widely used in groundwater remediation and wastewater treatment (Jiang et al., 2022). Fenton reagents were used by many researchers to simulate the ROS-induced ageing process of plastics (Zhang and Chen, 2020). Fenton reaction could age plastic products by producing reactive oxidants (·OH) through a mixture of H_2O_2 and Fe^{2+}. Liu et al. (2019) studied the ageing process of PS and PP microplastics by heat-activated $K_2S_2O_8$ and Fenton treatments, noting that the O/C ratio of the microplastics increased and the adsorption capacity was enhanced after ageing. Lang et al. (2020) examined the ageing behavior of PS MPs with H_2O_2 and Fenton reagents, and they pointed out that the aged microplastics will adsorb more heavy metals. Miao et al. (2020) investigated the degradation process of PVC by electro-Fenton-like technology with simultaneous cathodic reductive dechlorination and ·OH oxidation, achieving 75 % dechlorination efficiency and 56 % weight loss of PVC. Yang et al. (2022) investigated the degradation of PS microplastics by microbially driven Fenton reactions and indicated that ·OH could be continuously produced by microbially driven Fenton reactions in the environment. In fact, Fenton and Fenton like reactions widely exist in the atmosphere, rivers and marine environments. Therefore, rainwater facilities are inevitably affected by such rainwater and soil environment. However, most of the previous research only concentrated on laboratory standard microplastic spheres. The impacts of the Fenton reaction on rainwater facilities and the subsequent release of microplastics are still unknown.

In this study, Fenton ageing was applied to stimulate the ROS-induced ageing and microplastic release behavior of three typical plastic rainwater components, including rainwater pipe (mainly composed of polyvinyl chloride, PVC), modular storage tank (mainly composed of polypropylene, PP), and inspection well (mainly composed of high-density polyethylene, HDPE). The specific objectives are: i) to elucidate the surface and chemical changes of the plastic rainwater components during the ROS-induced ageing process in the rainwater environment; ii) to investigate the microplastic release behavior of the plastic rainwater components during ROS-induced ageing; and iii) to discover the mechanism of microplastic release which combined various characterization methods and material properties.

2. Material and methods

2.1. Sample preparation

Three typical plastic rainwater components made of different materials were selected as the experimental materials, including a HDPE rainwater

inspection well (Henan Huijie Pipe Industry Co., Ltd., China), a PP modular storage tank (Rainwater Keruiwo Co., Ltd., China), and a PVC rainwater pipe (Rainwater Keruiwo Co., Ltd., China). Sample blocks of 2 cm width ×6 cm length ×0.5 cm thickness (with surface area of 32 cm^2) were cut from these components, and weighed 5.66 ± 0.37 g, 3.87 ± 0.15 g, and 7.32 ± 0.61 g, respectively. The set of this sample size was based on the practical of the experiment to satisfy the detection limit. The sample blocks were washed with ultrapure water and a tube brush, then placed in a constant temperature drying oven at 40 °C for drying. The dried samples were stored in the dark pending use in the next step.

2.2. Ageing experiment

Fenton reagent was used to simulate the ROS-induced ageing behavior of plastic rainwater facilities in the natural environment and promote this process. Each gram of sample was blended in a 500 mL glass flask with 0.6 mL of H_2O_2 (30 %) and 38.8 mL of ultra-pure water, then 0.6 mL 200 mM Fe^{2+} was introduced (Liu et al., 2019). H_2O_2 or Fe^{2+} solutions were pre-adjusted at pH 4.0 to avoid the formation of ferric hydroxide under neutral and alkaline conditions that would inhibit the catalytic activity of Fe^{2+}. Equal doses of Fe^{2+} and H_2O_2 were injected every 12 h to maintain the oxidation of the microplastics (Liu et al., 2019). All the solutions were controlled at pH 4.0. The samples were shaken horizontally for 1, 3, and 6 days in a constant temperature shaking box (125 rpm). After shaking, the sample blocks were rinsed and collected, dried, weighed, and stored in the darkroom for further analysis. The solution in the conical flask is filtered by vacuum filtration and the glass fiber membranes (0.45 μm, Waterman GF/F) are subsequently dried for further analysis of the microplastic particles. Two controls were set in each group, both with Fenton reagent without the addition of sample blocks to ensure that the solutions were not contaminated during the experimental manipulation. All the experiments were conducted in triplicate.

2.3. Characterization of materials

2.3.1. Observation and identification

The influence of ageing on the morphological and chemical properties of the plastic rainwater components was characterized by a scanning electron microscope (SEM-EDX). Fourier transform infrared spectrometer (FTIR) was used to reveal the changes in chemical bonds on surfaces. The wavenumber range was set to 400–4000 cm^{-1} with a resolution of 4 cm^{-1}. 2D-COS analysis of the spectral data was performed to obtain synchronous and asynchronous spectra (Lasch and Noda, 2019). According to the research of Noda and Ozaki, the variation of the functional groups on the samples was determined (Noda, 2004). Qualitative analysis of carbon and oxygen on the surface of the sample blocks was conducted with XPS. The ·OH in the solution of ageing system for 10 min was detected and quantified using an electron paramagnetic resonance spectrometer (EPR, Bruker EMX-PLUS).

2.3.2. Characterization of released microplastics and data analysis

Microplastics on the dried filter membrane were observed and counted with an optical microscope (BOSMA606), and then combined with Nano Measurer 1.2 software for determining the size of those microplastics. The samples were prevented from dust contamination during the whole process. Statistical analysis was performed using SPSS software. The difference in microplastic release among different rainwater components and ageing degrees was tested by One-Way ANOVA, followed by Fisher's LSD post hoc test for multiple comparison ($p < 0.05$).

3. Results and discussion

3.1. Ageing behavior of plastic rainwater components

3.1.1. Surface morphology

Surficial structures of the rainwater components under different degrees of Fenton ageing are shown in Fig. 1. It's not surprising to find that the morphologies of the virgin materials were varied due to the difference in main components and production processes. With increasing ageing time from 0 to 6 days, the surface holes, fractures, and sharpness increased on the samples of the three facilities. As for the rainwater inspection well, HDPE was the main component. It can be observed that the surface became sharper under the erosion of free radicals, and the size of the cracks also increased. The variation of surface morphology of modular storage tanks with PP as the main component is also very evident. The surface became smoother and more delicate, with a large number of irregular folds and even small holes after 6 days. For the rainwater pipe, PVC was the main component, and more folds and cracks were observed after 6 days of ageing. Lang et al. (2020) examined the ageing process of PS spheres under H_2O_2 and Fenton ageing conditions and pointed out that ageing made the smooth spheres become rough and folded to different degrees, in which the Fenton reagent had a stronger oxidation ability than H_2O_2. Luo et al. (2021) investigated the ageing process of PE microplastics under ozone, Fenton, and heat-activated persulfate treatments, and pointed out that the aged microplastic surface showed significant fragmentation and cracking and exhibited more layered structures. In our previous study, after 45 days of UV ageing, the surface holes, fractures, and roughness increased in all

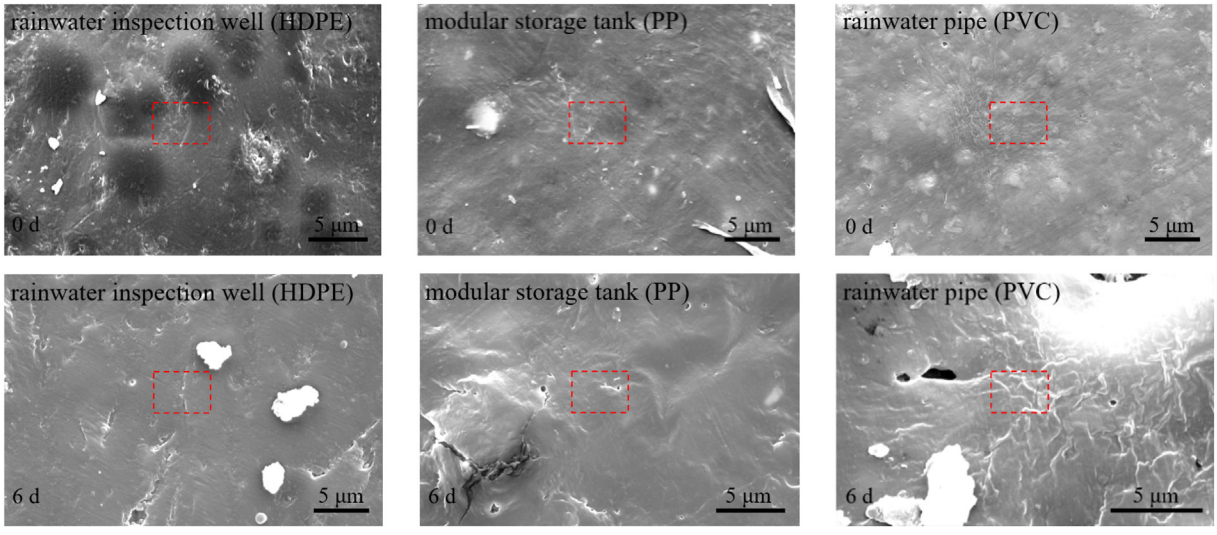

Fig. 1. SEM images of sample blocks from rainwater facilities before ageing (0 d) and after 6 days of Fenton ageing.

three facilities samples, while the surface of the samples decreased in roughness and became smoother and sharper after Fenton ageing in the present study. As observed in the area within the red frame, a large number of small bulges and folds on the surface of the sample after ageing is replaced by larger cracks and smooth surfaces, the indication of free radical erosion of the surface of the rainwater facility. These results suggest that the Fenton reagent could cause much more severe structural degradation and a much more significant release of microplastic than UV ageing.

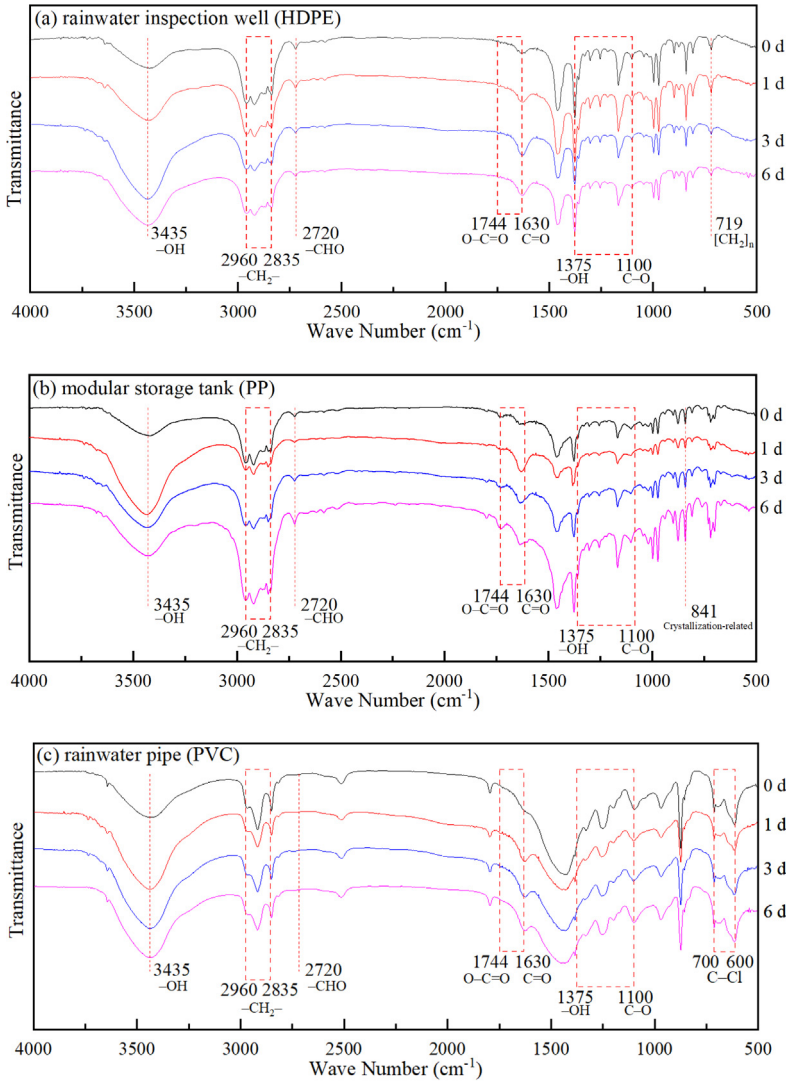

A. FTIR spectra of the rainwater components.

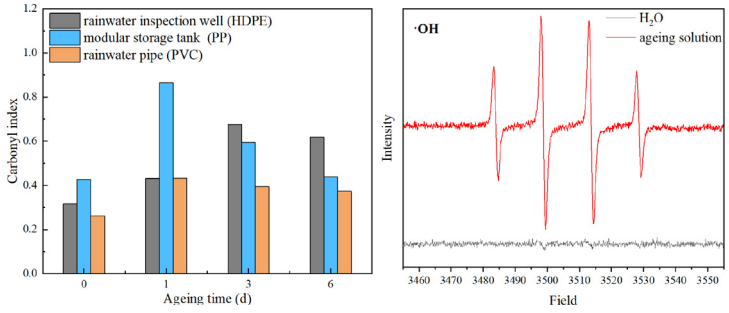

B. Carbonyl index of the three rainwater facilities

C. EPR result of ·OH in the simulated ageing system.

Fig. 2. FTIR spectra of the three rainwater components' surface layers under Fenton ageing and EPR result of ·OH in the simulated ageing system.
A. FTIR spectra of the rainwater components.
B. Carbonyl index of the three rainwater facilities.
C. EPR result of ·OH in the simulated ageing system.

Furthermore, the surfaces of all three materials were irregular with different degrees of cracking before the ageing treatment, which could be related to the production process, additive ratios, and storage environment (Matias et al., 2020; Gould et al., 2013).

In summary, the Fenton ageing caused significant morphological changes in the three rainwater facilities. Along with cracks and folds increasing, the surface became smoother due to the detachment of surface particles, which indicates that more microplastics might be released during the Fenton ageing process.

3.1.2. FTIR analysis and EPR test

As shown in Fig. 2 (A), the intensity of the spectral bands associated with the oxygen-containing functional groups in the surface layer of the three rainwater components increased during Fenton ageing, and the area of the peaks increased. The change of the carbonyl group (C = O) in the FTIR spectrum at 1630 cm^{-1} was an important sign of the change in the oxygen-containing functional group, and the intensity was positively correlated with the generation of the carbonyl group (Almond et al., 2020). In addition, the observed absorption peaks at 2720 cm^{-1} of –CHO (in the HDPE inspection well and PP modular storage tank), 1744 cm^{-1} of O–C = O (in the PP modular storage tank), and 1100 cm^{-1} of C—O (in the HDPE inspection well, PP modular storage tank, and PVC rainwater pipe) increased and expanded similarly during the ageing process. The change in the modular storage tank (PP) was the most obvious, and a newly formed absorption peak (1744 cm^{-1}, O–C = O) could be observed. In the same way, the hydroxyl (–OH) peaks at around 3435 cm^{-1} and 1375 cm^{-1} of the three materials also tended to increase and expand over ageing time, which was consistent with the change in the –OH peak during the degradation of PE mulching film by bacterial strains (Yin et al., 2020). Lang et al. (2020) investigated the spectral change of standard sphere PS microplastics during the Fenton ageing process and noted that the absorption bands of several oxygen-containing functional groups (C–OH, O–C = O, C═O, C–O–C) also strengthened and widened along increasing ageing time, which is similar with our observations. In the ageing process, plastic rainwater facilities are gradually oxidized and polymer chains break irregularly. Because of the lower bond energy, the breakage of side groups and substituents/side chains occurs initially. The C—H bond breaks first, forming oxygen-containing functional groups C—O, C–OH, and then generating C═O while carbon chains are further broken. This process could promote the release of microplastics, thus C═O is commonly accepted as an indicator of plastic ageing.

The carbonyl funtional group is the indicator of ageing degree, and it is also the final product of ageing process. And the carbonyl index was calculated from the ratio between the integration of the carbonyl and methylene absorbance bands, to further determine the ageing degree of the plastic samples (Almond et al., 2020). As shown in Fig. 2 (B), the carbonyl index of rainwater facilities increased after Fenton ageing, then slightly decreased or leveled off after reaching a plateau. It could result from the exposure of the less degraded inner layer due to the erosion of the oxidized surface. By correlating the changes in the release process, it can be found that the larger the maximum value of the carbonyl index, the higher the final microplastic release and the highest release rate. Therefore, with the rapid increase of microplastic release, it may be an important reason for the decrease of carbonyl index. Among them, the modular storage tank (PP) changed most obviously. The changing behavior of the carbonyl index is related to the size and structural changes of plastics. For example, Toapanta et al. (2021) investigated the photoageing behavior of bead and fragment polypropylene microplastics and found that the carbonyl index of small-sized microplastics (250–500 μm) gradually increased during ageing and then reached a plateau. On the contrary, the carbonyl index of large-sized (500–1000 μm) microplastics exhibited a significant decrease during ageing, which was due to the erosion of the oxidized surface and exposure of the inner layer that had a lower degree of ageing.

The average carbonyl index during the 6 days of Fenton ageing was 0.536 (i.e., 0.375–0.865), which was significantly higher than that (0.310–0.442) of 15–45 days of UV ageing in our previous study (Zhang et al., 2022). This implies that ROS has a greater impact on the ageing of rainwater facilities than UV ageing. Consequently, they are more likely to release microplastics and additives to the environment under ROS oxidation.

Similarly, in order to reveal the changes in other oxygen-containing functional groups (such as C–OH and C—O bonds) during the ageing process, the correlation index was obtained using the same method to compare the integration of methylene absorbance bands, as shown in Fig. S1. It can be observed that the ratio of C–OH, and C—O on the surface of the rainwater facility increases with ageing. However, the change of both indices is relatively weak, where the C–OH and C—O index of the modular storage tank is closer to the change of the carbonyl index.

The EPR spectrum of ·OH in the simulated ageing solution in the system is shown in Fig. 2(C). According to relevant studies, the main reactive oxygen species (ROS) produced in the aqueous reaction (i.e., Fenton reaction) between divalent iron and H_2O_2 are high-valent iron (IV) oxide substances (Chen, 2019). Its further conversion of these substances to hydroxyl radicals occurs when ·OH has the maximum oxidation potential under acidic conditions and dominates the reaction process. Rainwater facilities will inevitably contact with free radicals in the natural environment, causing ageing of plastic facilities. Firstly, ·OH breaks the C − H of the polymer and generates alkyl radicals (R·), followed by the generation of alkoxy groups (RO·); eventually, alkoxy groups (RO·) combine with hydrogen and form hydroxyl functional groups, or generate carbonyl groups through disproportionation reactions. And the carbonyl group formation process occurs with a large number of chain breaks, thus accelerating the release of microplastics from rainwater facilities.

And the presence of ROS in the environment is extremely widespread. Song et al. (2022) studied the concentration of ROS in Poyang Lake during flood and drought periods, where the concentration of ·OH was (1.58–1.75) × 10^{-16} M. In this study, the total spin of EPR inferred that the concentration of ·OH in solution concentration was 1.51 × 10^{-6} M (1.232 × 10^{13} spins).

3.1.3. 2D-COS analysis

The 2D-COS maps (Fig. 3) were obtained by further analysis of the fingerprint region to reveal changes in functional groups on the surface. The autocorrelation peaks on the diagonal of the synchronous correlation spectra can reflect the degree of functional groups affected by external perturbations. The cross peaks on the non-diagonal can reflect the similarity changes in the intensity of different wave number spectra. The asynchronous correlation spectra are mainly used to distinguish the sources of the spectral peaks and the masked overlapping peaks. The order of changes in different wave number groups can be judged by comparing the cross peaks of the synchronous and asynchronous correlation spectra. Five correlation bands (1100, 1300, 1375, 1630, 1744 cm^{-1}) were chosen to uncover sequence changes in the functional groups (C—C, C—O, O–C = O, C–OH, C═O). For the three types of facilities, the positive and negative variations of the corresponding absorption bands in the synchronous and asynchronous correlation spectra are listed in Table 1.

Through the positive correlation of the cross-peaks in the synchronous correlation bands for the five types of chemical bonds, the distribution of the peaks of the three facilities can be found to be almost similar. The modular storage tank (PP) had the largest spectral variation range, which may result in the maximum release of microplastics. The change in functional group intensity of rainwater pipe (PVC) was the most significant, and the changes in the surface morphology were also the most obvious.

However, the sequence of functional group changes of the three materials was different. The functional group changes of the inspection well (HDPE) and rainwater pipe (PVC) occurred in the order of 1100 (C − O) > 1375 (C − OH) > 1300 (C − C). The changes in the surface functional groups of the modular storage tank (PP) followed in the order of 1630 (C = O) > 1375 (C − OH) >1100 (C − O). The differences in the surface functional groups may be caused by the obvious increase of microplastic release from the modular storage tank (PP) with increasing ageing time, resulting in the rapid peeling of microplastics on the surface. The impact of Fenton ageing

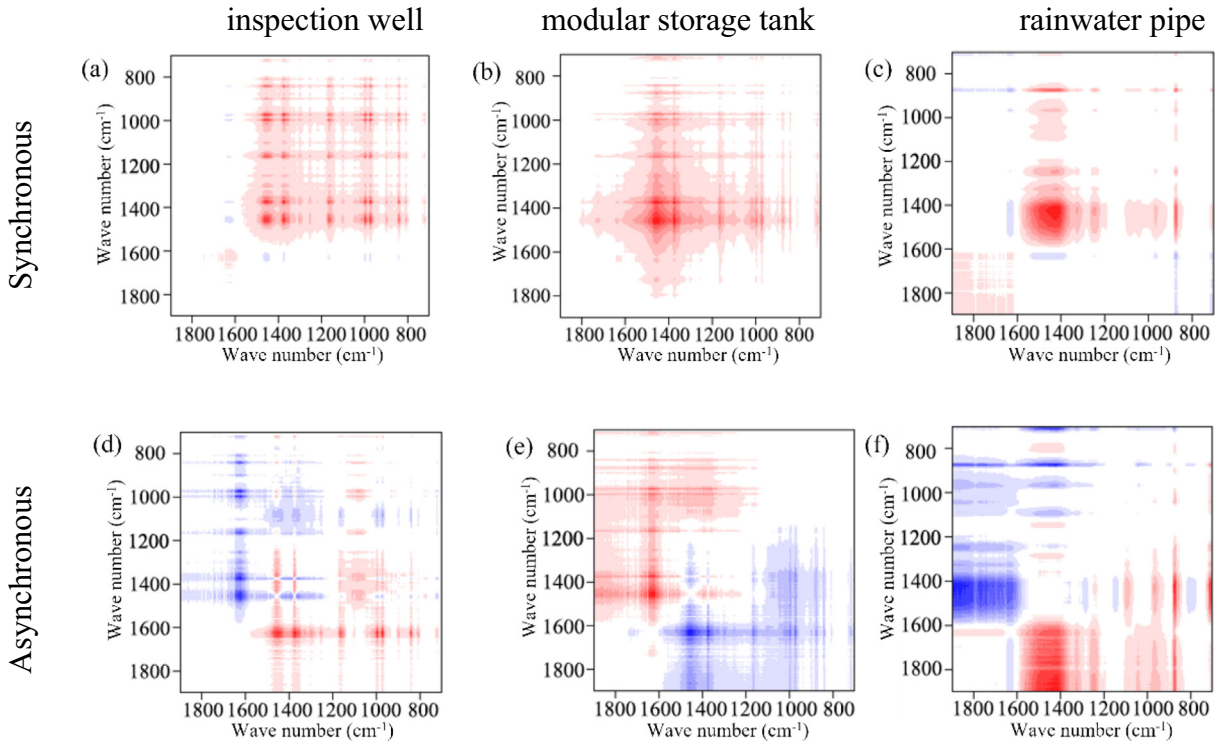

Fig. 3. The 2D-COS map of rainwater facilities after 6 days of Fenton ageing. Red and blue colors in the graph indicate positive and negative correlations, respectively.

on the three materials is greatly different from UV ageing (Zhang et al., 2022), where the wavenumber range affected on the surface functional groups of the rainwater inspection well (HDPE) and modular storage tank (PP) increased, while the functional groups of the rainwater pipe (PVC) exhibit that the lower wavenumber range (1000–1200 cm^{-1}) decreases and the higher wavenumber range (1800–1900 cm^{-1}) increases. In addition, the asynchronous spectra of the three components exhibited richer information.

3.1.4. XPS analysis

The sample surface was characterized by XPS, and the change in chemical bond was further revealed by analysing XPS deconvolution data. The results are shown in Fig. 4. The functional groups of the inspection well (HDPE) and modular storage tank (PP) changed obviously after 6 days of ageing. There was a C—O peak at 286.23 eV for the inspection well (HDPE), and the intensity of the C═O peak was enhanced at 287.53 eV. In the spectrum of the modular storage tank (PP), a weak C═O peak was observed. The decrease in the intensity of C = C/C–C/C–H and the increase in the intensity of the C═O peak indicate the appearance of oxygen groups and the breakage of the backbone (Miao et al., 2020). However, there was no new peak generated in the rainwater pipe (PVC). The peak of O–C = O existed in all the materials before and after ageing, which could most likely originate from one of the most widespread plasticizers (i.e., phthalates) (Suhrhoff and Scholz-Böttcher, 2016). The surface elements were semi-quantitatively analyzed by XPS, and the results are shown in Table 2. Ca, Si, and Cl elements in the aged rainwater pipe (PVC) were significantly decreased, indicating that the oxidation by ROS could lead to the decomposition and release of other additives chemicals (antioxidants-phenolic compounds, flame retardants-brominated flame retardants, photostabilizers-benzotriazoles and plasticizers-phthalates) from rainwater facilities. The release of additives in plastic products can cause surface defects and increase the risk of microplastic release. The presence of oxygen containing additive might influence the ageing process. Since the additives amount added in the samples is quite small (<10 % of the total components, according to the manufacture), we assume that the additives might exert limited influence on ageing process compared with the main components. To distinguish to what extent of the additives influence the ageing, further study remains to be conducted.

Besides that, the decrease of Cl elements could be due to the depolymerization and dichlorination of PVC rainwater pipes occurs with the ageing process. Compared with UV ageing (Zhang et al., 2022), the differences in functional groups and elemental changes on the surfaces of the inspection well (HDPE) and the modular storage tank (PP) were similar, while the rainwater pipe (PVC) was more seriously influenced by UV radiation, with more types of oxygen-containing functional groups.

3.2. Microplastic release behavior

3.2.1. Release of microplastics

Fig. 5 shows the microplastics released from the rainwater components before and after Fenton ageing. The released microplastics were irregular fragments and particles that were basically black, brown, and transparent in color. The morphological characteristics of the released microplastics

Table 1
Synchronous (Φ) and asynchronous (Ψ, in the brackets) 2D–COS data for the sign of each cross peak in the maps of the three rainwater components.

Wavenumber (cm^{-1})	Band	Inspection well				Modular storage tank				Rainwater pipe			
		1100	1300	1375	1630	1100	1300	1375	1630	1100	1300	1375	1630
1100	C–O	+ (0)	+ (−)	+ (−)	0	0	0	+ (+)	0	0	0	+ (−)	0
1300	C–C		+ (0)	+ (+)	0		+ (0)	+ (0)	+ (+)		0	+ (+)	0
1375	C–OH			+ (0)	0			+ (0)	+ (+)			+ (0)	0
1630	C = O				+ (0)				+ (0)				+ (0)

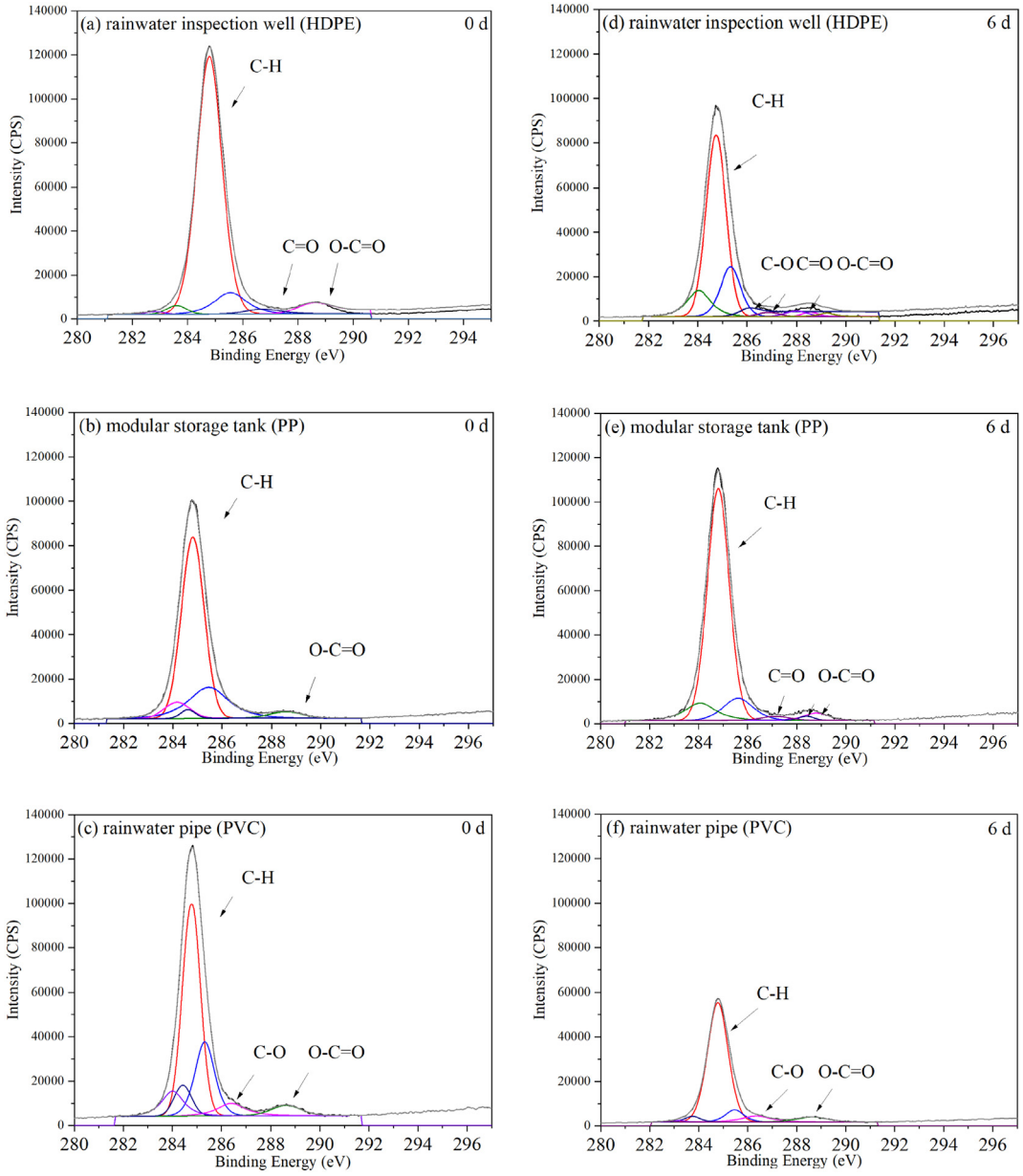

Fig. 4. X-ray photoelectron spectra (XPS) of rainwater facilities without ageing (0 d, a–c) (Zhang et al., 2022) and after 6 days of Fenton ageing (d–f).

were observed by SEM, and it was found that the irregularity of the morphology of the released microplastics increased, the edges became sharp, and the surface bulged after ageing. Fadare et al. (2020) investigated the phenomenon of microplastic release from plastic food containers and noted that the shapes of particles could be classified as cubic, spherical, rod-like, and irregular shapes. Similar to our previous research, the shapes of the released microplastics were all irregular particles and fragments (Zhang et al., 2022), but the surfaces of the released microplastics were smoother and the edges were sharper after Fenton ageing.

3.2.2. The change in the amount of microplastics

Fig. 6 shows the amounts of microplastics released from the three rainwater components under Fenton ageing. With increasing degradation, three types of rainwater facilities release increasing amounts of microplastics.

Table 2
Semi-quantitative analysis of XPS surface elements.

	Rainwater components	Elements Atomic%									
		C	O	Ca	Si	S	Cl	N	Ag	Cd	other
Pristine (Zhang et al., 2022)	Inspection well	82.82	12.82	2.08	2.28	–	–	–	–	–	–
	Modular storage tank	74.06	17.00	1.85	3.22	2.22	–	1.64	–	–	0.01
	Rainwater pipe	82.44	11.04	1.80	1.83	–	1.53	1.31	0.04	–	0.01
Fenton ageing	Inspection well	80.44	14.75	1.64	3.10	–	–	–	0.04	–	0.03
	Modular storage tank	84.88	11.79	0.77	2.02	0.52	–	–	–	0.02	–
	Rainwater pipe	85.9	11.63	–	1.02	–	1.43	–	–	0.02	–

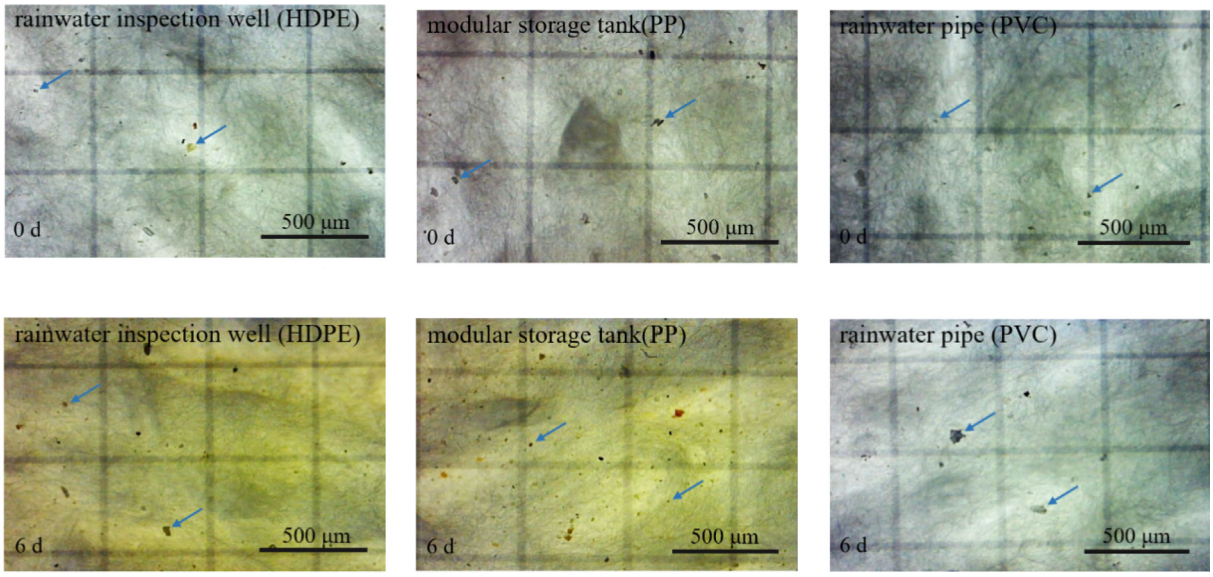

A. Microscopic images of the released microplastics on glass fiber filters.

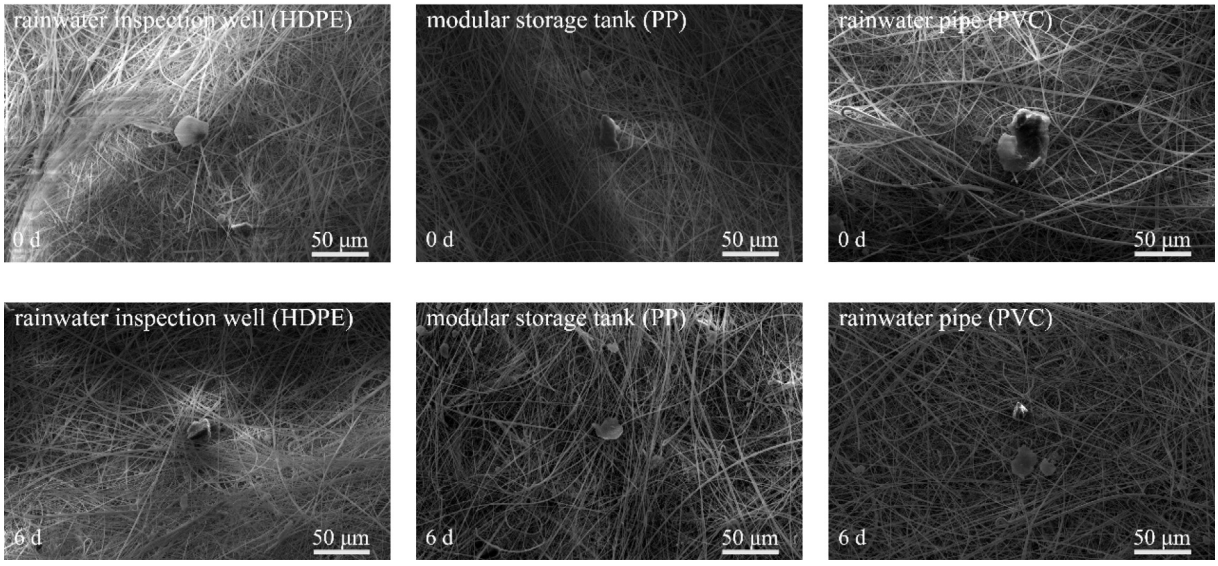

B. SEM images of the released microplastics.

Fig. 5. Microscopic images of the released microplastics from the rainwater inspection well, modular storage tank, and rainwater pipe before (0 d) and after 6 days of Fenton ageing.
A. Microscopic images of the released microplastics on glass fiber filters.
B. SEM images of the released microplastics.

The microplastic release from the modular storage tank (PP) was the highest among the three facilities for days 1 to 6 of the ageing process (Fig. 6a), rising from 323 ± 93 to 6617 ± 928 items/g, followed by the inspection wells (HDPE), which ranged from 1215 ± 164 to 6196 ± 862 items/g. The least amount (158 ± 50 to 1377 ± 460 items/g) of release from rainwater pipes (PVC). As a result, the risk of microplastic release is more severe for rainwater inspection wells and storage tanks as compared to rainwater pipes, which have a relatively low risk of microplastic release for the same ageing time. It is evident that the amount of microplastic released is largely dependent on the main composition of the material, except for the operating environment of the rainwater facility. The average amount of microplastics released from the inspection well (3186 items/g) and the modular storage tank (3326 items/g) within 6 days of ageing was much higher than that of the rainwater pipe (693 items/g), which indicates that the inspection well and the modular storage were more vulnerable to the influence of Fenton ageing. Interestingly, all three rainwater facilities showed a significant positive correlation between the number of microplastics released and ageing time (r^2 = 0.915, 0.935, and 0.994, respectively, Fig. 6b). This phenomenon might be related to the reduction of crystallinity and stability of the plastic facility after 6 days of ageing.

The quantity of microplastics released from Fenton-aged rainwater facilities is much greater than those of plastics in everyday products. Fadare et al. (2020) investigated the process of microplastic release from consumer plastic food containers (take away pack) and pointed out that the release of microplastics from the containers was 18 ± 4 mg/pack. Kutralam-Muniasamy et al. (2020) detected 23 milk samples from 8 brands,

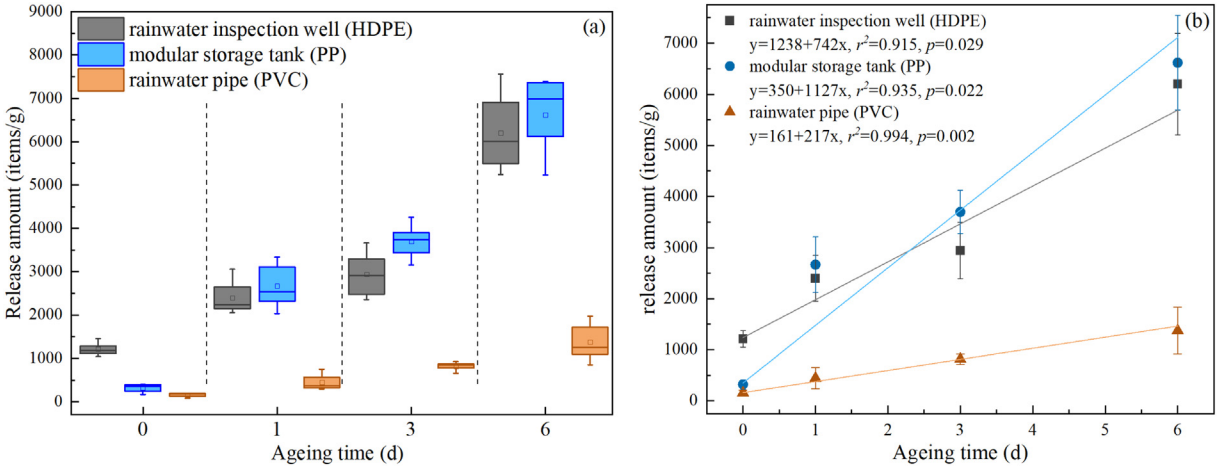

Fig. 6. Microplastic released from rainwater facilities, and correlation analysis between the release amount and ageing time.

and the concentration of microplastic was 6.5 ± 2.3 items/L. It was pointed out that the common types of microplastic came from the membrane materials in dairy processes. Chen et al. (2021) reported that the abundance of microplastics in construction site soil covered with anti-dust nets was 4069 items/kg above that of uncovered soils. Therefore, the risk of microplastic pollution from plastic rainwater facilities should be taken seriously. As a key component of urban rainwater facilities, the microplastics released from plastic inspection wells and storage tanks will migrate to the surrounding soil and water bodies, which has potential harm to the ecological environment.

3.2.3. Size distribution

The size distribution of the released microplastics is shown in Fig. 7. The changes in particle size were similar and mostly concentrated in the size of <30 μm (78.1 %). This proportion was larger than that of UV ageing in our previous study, with <30 μm accounting for only 64.3 % (Zhang et al., 2022). Therefore, the microplastic particle size <30 μm increased obviously with the increasing ageing degree of plastic rainwater facilities. The microplastics with a size <30 μm released from the inspection well (HDPE) increased by 11 %, and the number of microplastics with a size of >50 μm decreased by 7 %. However, the microplastics with the size <10 μm and >50 μm released from the modular storage tank (PP) decreased by 3 % and 5 %, and the number of microplastics with the size of 10–30 μm increased by 13 %. As for the rainwater pipes (PVC), the results are similar to those of rainwater inspection wells, but with a broader range of variation. The microplastic with a size of <30 μm increased by 36 %, and the number of microplastics with a size of >50 μm decreased by 26 %. Wang et al. (2021) studied microplastic release from disposable masks under ultraviolet light weathering and pointed out that the particle size was primarily concentrated between 10 and 20 μm and 50–250 μm.

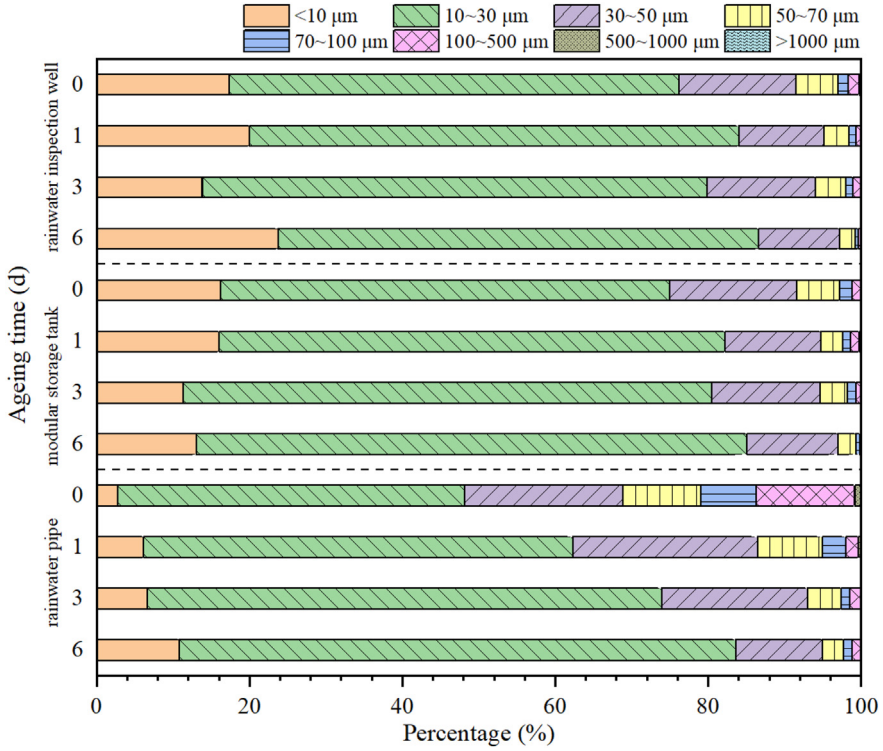

Fig. 7. Size distribution of released microplastics.

Mason et al. (2018) detected 11 brands of bottled water from 9 countries and 93 % of the samples showed evidence of microplastic contamination, which was mainly in the particle size range of 6.5 to 100 μm. Polypropylene was the most common polymer type (54 %). Li et al. (2020) selected ten representative PP infant feeding bottles and tested their microplastic release behavior under different water temperatures, sterilization, and repeated use. It was found that the baby bottles would release a large amount of microplastics, and the particle size is concentrated in the 0.8–10 μm range. Ranjan et al. (2021) researched the mechanism of microplastic release from the hydrophobic film within disposable paper cups and pointed out that the released microplastics are <10 μm in particle size. Su et al. (2022) examined the behavior of microplastic release from infant pacifiers by steam sterilization and noted that most of the microplastics were 1.5–10 μm in size (roughly 81 %). Thus, in general, microplastics released from plastic rainwater facilities have relatively bigger particle sizes than those of food-grade plastic products.

Moreover, it can be observed that the change in particle size of PVC rainwater pipe before and after ageing is the most significant, however, the difference in particle size distribution of microplastics in the three plastic facilities aged to 6 days is smaller. By combining the changes of microplastic release (Fig. 6) and particle size (Fig. 7), it is probably due to the non-uniformity of the surface of the facilities in the initial stage of ageing, the larger microplastic particles peel off first, making the surface defective, and then a large amount of small particle size microplastic release occurs. This should be the typical stage of microplastic release from plastic facilities, except that the inspection well and modular storage tank experienced this stage earlier and are not reflected in the graph.

3.2.4. Correlation between release amount and particle size

An overview of the microplastic release behavior and size distribution over ageing time is given in Fig. 8a. The particle size of the released microplastics ranged from 2 to 1362 μm, of which the largest proportion (62.7 %) was in 10–30 μm. In general, during the Fenton ageing process, the amount of the released microplastics increased over time. Meanwhile, the particle size distribution changed significantly, and the proportion of small-sized microplastics (0–30 μm) increased the most. As the particle size of microplastics decreases, it will cause more harm to the ecological environment.

Considering the differences caused by the microplastic release statistics, in addition to the microplastic release per unit mass of the rainwater facilities, the microplastic release per unit area of the rainwater facilities was likewise obtained (Fig. S2). Taking the microplastic release per unit area as the measure, it can be seen that the microplastic release of the three rainwater facilities is between 73 and 1063 items/cm^2, in the order of modular storage tank > inspection well > rainwater pipe. And due to the high density and smaller surface area/mass ratio of PVC rainwater pipes, they exhibit a stronger risk of microplastic release.

It is noteworthy that the quantity increased exponentially with decreasing particle size, and the longer the ageing time, the faster the increase (Fig. 8b). Compared with previous studies (e.g., UV ageing), which showed that microplastic release could be inhibited by factors such as cross-links along with ageing, the release of microplastics with different particle sizes kept increasing under the Fenton ageing process. This may suggest that the mechanism of Fenton ageing is different from that of other ageing processes (e.g., UV ageing) (Zhang et al., 2022).

4. Conclusion

As an integral part of the modern rainwater system, it is of crucial importance to analyze the microplastic release behavior from plastic rainwater components to prevent microplastic pollution. In this study, the microplastic release behavior of three typical plastic rainwater components under the effect of reactive oxygen species (ROS) was investigated by the Fenton ageing method, which combined the surface characteristics of the ageing materials and the released microplastics.

As the time of ageing increases, fractures, wrinkles, and holes develop on the surface of plastic rainwater facilities. Meanwhile, the surface became sharper. The Fenton ageing process leads to increased oxygen-containing functional groups, increased carbonyl index, and broken carbon chains on the surface of the rainwater facilities, which accelerated the release of microplastics. XPS showed that the carbon and oxygen functional group species of rainwater inspection well (HDPE) and modular storage tank (PP) increased after Fenton ageing, but rainwater pipes (PVC) were the most stable, with less change in functional groups and the least release of microplastics. For these three facilities, the quantity of microplastic released ranged from 158 to 6617 items/g, as follows: modular storage tanks (PP) > rainwater inspection wells (HDPE) > rainwater pipes (PVC). The proportion of released microplastics with sizes of 10–30 μm increased significantly, while the size of microplastics larger than 30 μm decreased. The most significant change was observed in the rainwater pipe, followed by the modular storage tank and the rainwater inspection well. The microplastics released from rainwater facilities have significantly larger

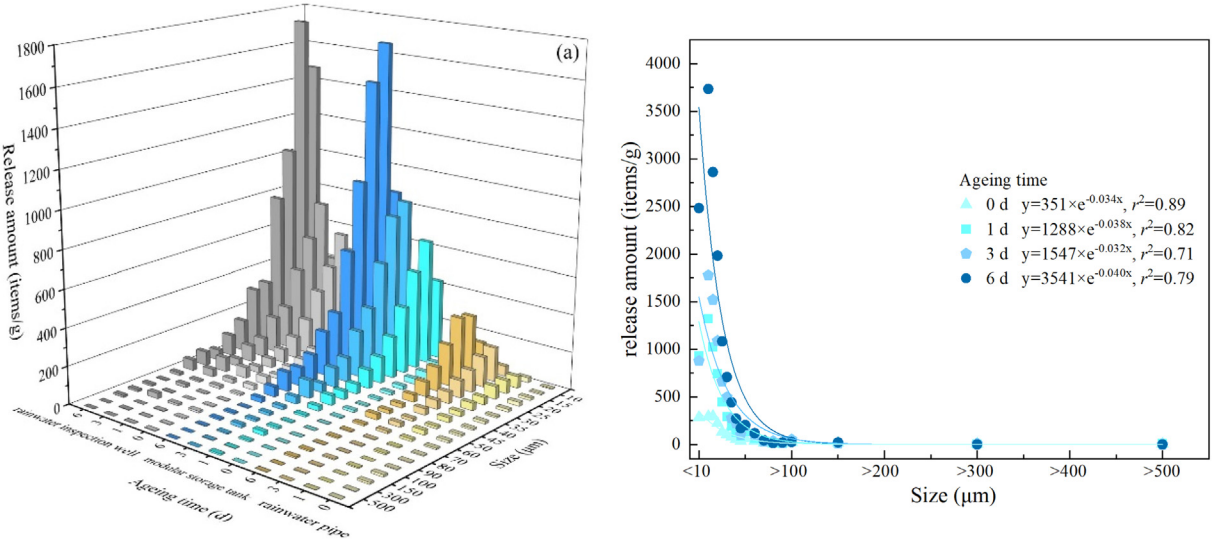

Fig. 8. Changes and correlation analysis between the release amount and particle size of microplastics before (0 d) and after 1 d, 3 d, and 6 d of Fenton ageing. The left graph (a) shows the three-dimensional relationship between microplastic release, size and ageing time; the right graph (b) shows the change characteristics of microplastic particle size with ageing time.

sizes than food-grade plastic products with more complex surface properties. The particle size of 10–30 μm accounts for the most (62.7 %). As shown from our results, microplastic pollution from plastic rainwater facilities under ROS-induced ageing should be taken seriously. Further attention should be paid to the ageing effect of ROS on plastic facilities in the water environment to enhance the prevention and control of microplastic pollution.

CRediT authorship contribution statement

Chao Liu: Investigation, Data curation, Visualization, Writing-Original draft, Formal analysis. **Xiaoran Zhang**: Conceptualization, Methodology, Data curation, Writing-Original draft, Formal analysis, Funding acquisition. **Junfeng Liu**: Data curation, Writing-Reviewing and Editing. **Zhifei Li**: Validation, Resources. **Ziyang Zhang**: Data analysis. **Yongwei Gong**: Methodology, Validation. **Xiaojuan Bai**: Methodology, Validation. **Chaohong Tan**: Characterization analysis. **Haiyan Li**: Validation, Funding acquisition. **Junqi Li**: Validation. **Yuansheng Hu**: Conceptualization, Revision.

Data availability

Data will be made available on request.

Declaration of competing interest

The authors declare that they have no known competing financial interests or personal relationships that could have appeared to influence the work reported in this paper.

Acknowledgements

This research was supported by The Construction of High Level Teaching Teams in Universities of Beijing–the Youth Top–Notch Talent Cultivation Program (CIT&TCD201804051); National Natural Science Foundation of the China (51508017); The Youth Beijing Scholars Program (No. 024).

Appendix A. Supplementary data

Supplementary data to this article can be found online at https://doi.org/10.1016/j.scitotenv.2023.161397.

References

Almond, J., Sugumaar, P., Wenzel, M.N., Hill, G., Wallis, C., 2020. Determination of the carbonyl index of polyethylene and polypropylene using specified area under band methodology with ATR-FTIR spectroscopy. e-Polymers 20 (1), 369–381. https://doi.org/10.1515/epoly-2020-0041.

Bai, X., Ma, W., Zhang, Q., Zhang, L., Zhong, S., Shu, X., 2022. Photon-induced redox chemistry on pyrite promotes photoaging of polystyrene microplastics. Sci. Total Environ. 829, 154441. https://doi.org/10.1016/j.scitotenv.2022.154441.

Chen, H.Y., 2019. Why the reactive oxygen species of the Fenton reaction switches from oxoiron (IV) species to hydroxyl radical in phosphate buffer solutions?A computational rationale. ACS Omega 4 (9), 14105–14113. https://doi.org/10.1021/acsomega.9b02023.

Chen, Y., Wu, Y., Ma, J., An, Y., Liu, Q., Yang, S., Tian, Y., 2021. Microplastics pollution in the soil mulched by dust-proof nets: a case study in Beijing, China. Environ. Pollut. 275, 116600. https://doi.org/10.1016/j.envpol.2021.116600.

Duan, J., Li, Y., Gao, J., Cao, R., Shang, E., Zhang, W., 2022. ROS-mediated photoaging pathways of nano-and micro-plastic particles under UV irradiation. Water Res. 118320. https://doi.org/10.1016/j.watres.2022.118320.

Eom, H.J., Haque, M.N., Lee, S., Rhee, J.S., 2021. Exposure to metals premixed with microplastics increases toxicity through bioconcentration and impairs antioxidant defense and cholinergic response in a marine mysid. Comp. Biochem. Physiol. C: Toxicol. Pharmacol. 249, 109142. https://doi.org/10.1016/j.cbpc.2021.109142.

Fadare, O.O., Wan, B., Guo, L.H., Zhao, L., 2020. Microplastics from consumer plastic food containers: are we consuming it? Chemosphere 253, 126787. https://doi.org/10.1016/j.chemosphere.2020.126787.

Gali, N.K., Stevanovic, S., Brimblecombe, P., Brown, R.A., Ristovski, Z., Ning, Z., 2020. The diurnal characteristics of PM-bound ROS and its influencing factors at urban ambient and roadside environments. Atmos. Res. 244, 105039. https://doi.org/10.1016/j.atmosres.2020.105039.

Gould, S.J., Davis, P., Beale, D.J., Marlow, D.R., 2013. Failure analysis of a PVC sewer pipeline by fractography and materials characterization. Eng. Fail. Anal. 34, 41–50. https://doi.org/10.1016/j.engfailanal.2013.07.009.

Han, R., Lv, J., Zhang, S., Wang, Z., Li, G., Zhang, S., 2022b. Dithionite extractable iron responsible for the production of hydroxyl radicals in soils under fluctuating redox conditions. Geoderma 415, 115784. https://doi.org/10.1016/j.geoderma.2022.115784.

Han, R., Wang, Z., Lv, J., Zhu, Z., Yu, G.H., Li, G., Zhu, Y.G., 2022a. Multiple effects of humic components on microbially mediated iron redox processes and production of hydroxyl radicals. Environ.Sci.Technol. https://doi.org/10.1021/acs.est.2c03799.

Hu, K., Yang, Y., Zuo, J., Tian, W., Wang, Y., Duan, X., Wang, S., 2022. Emerging microplastics in the environment: properties, distributions, and impacts. Chemosphere 134118. https://doi.org/10.1016/j.chemosphere.2022.134118.

Jiang, Q., Li, Z., Cui, Z., Wei, R., Nie, K., Xu, H., Liu, L., 2021. Quantum mechanical investigation of the oxidative cleavage of the C-C backbone bonds in polyethylene model molecules. Polymers 13 (16), 2730. https://doi.org/10.3390/polym13162730.

Jiang, Y., Ran, J., Mao, K., Yang, X., Zhong, L., Yang, C., Zhang, H., 2022. Recent progress in Fenton/Fenton-like reactions for the removal of antibiotics in aqueous environments. Ecotoxicol. Environ. Saf. 236, 113464. https://doi.org/10.1016/j.ecoenv.2022.113464.

Kutralam-Muniasamy, G., Pérez-Guevara, F., Elizalde-Martínez, I., Shruti, V.C., 2020. Branded milks–are they immune from microplastics contamination? Sci. Total Environ. 714, 136823. https://doi.org/10.1016/j.scitotenv.2020.136823.

Lang, M., Yu, X., Liu, J., Xia, T., Wang, T., Jia, H., Guo, X., 2020. Fenton aging significantly affects the heavy metal adsorption capacity of polystyrene microplastics. Sci. Total Environ. 722, 137762. https://doi.org/10.1016/j.scitotenv.2020.137762.

Lasch, P., Noda, I., 2019. Two-dimensional correlation spectroscopy (2D-COS) for analysis of spatially resolved vibrational spectra. Appl. Spectrosc. 73 (4), 359–379. https://doi.org/10.1177/0003702818819880.

Li, D., Shi, Y., Yang, L., Xiao, L., Kehoe, D.K., Gun'ko, Y.K., Wang, J.J., 2020. Microplastic release from the degradation of polypropylene feeding bottles during infant formula preparation. Nat. Food 1 (11), 746–754. https://doi.org/10.1038/s43016-020-00171-y.

Li, X., Li, M., Mei, Q., Niu, S., Wang, X., Xu, H., Zhou, J.L., 2021. Aging microplastics in wastewater pipeline networks and treatment processes: physicochemical characteristics and cd adsorption. Sci. Total Environ. 797, 148940. https://doi.org/10.1016/j.scitotenv.2021.148940.

Liu, P., Qian, L., Wang, H., Zhan, X., Lu, K., Gu, C., Gao, S., 2019. New insights into the aging behavior of microplastics accelerated by advanced oxidation processes. Environ.Sci. Technol. 53 (7), 3579–3588. https://doi.org/10.1021/acs.est.9b00493.

Liu, P., Li, H., Wu, J., Wu, X., Shi, Y., Yang, Z., Gao, S., 2022. Polystyrene microplastics accelerated photodegradation of co-existed polypropylene via photosensitization of polymer itself and released organic compounds. Water Res. 214, 118209. https://doi.org/10.1016/j.watres.2022.118209.

Luo, H., Zeng, Y., Zhao, Y., Xiang, Y., Li, Y., Pan, X., 2021. Effects of advanced oxidation processes on leachates and properties of microplastics. J. Hazard. Mater. 413, 125342. https://doi.org/10.1016/j.jhazmat.2021.125342.

Mason, S.A., Welch, V.G., Neratko, J., 2018. Synthetic polymer contamination in bottled water. Front.Chem. 407. https://doi.org/10.3389/fchem.2018.00407.

Matias, Á.A., Lima, M.S., Pereira, J., Pereira, P., Barros, R., Coelho, J.F., Serra, A.C., 2020. Use of recycled polypropylene/poly (ethylene terephthalate) blends to manufacture water pipes: an industrial scale study. Waste Manag. 101, 250–258. https://doi.org/10.1016/j.wasman.2019.10.001.

Miao, F., Liu, Y., Gao, M., Yu, X., Xiao, P., Wang, M., Wang, X., 2020. Degradation of polyvinyl chloride microplastics via an electro-Fenton-like system with a TiO2/graphite cathode. J. Hazard. Mater. 399, 123023. https://doi.org/10.1016/j.jhazmat.2020.123023.

Miranda, M.N., Sampaio, M.J., Tavares, P.B., Silva, A.M., Pereira, M.F.R., 2021. Aging assessment of microplastics (LDPE, PET and uPVC) under urban environment stressors. Sci. Total Environ. 796, 148914. https://doi.org/10.1016/j.scitotenv.2021.148914.

Morris, J.J., Rose, A.L., Lu, Z., 2022. Reactive oxygen species in the world ocean and their impacts on marine ecosystems. Redox Biol. 102285. https://doi.org/10.1016/j.redox.2022.102285.

Murphy, S.A., Meng, S., Solomon, B.M., Dias, D.M., Shaw, T.J., Ferry, J.L., 2016. Hydrous ferric oxides in sediment catalyze formation of reactive oxygen species during sulfide oxidation. Front. Mar. Sci. 3, 227. https://doi.org/10.3389/fmars.2016.00227.

Nielsen, A.H., Vollertsen, J., Jensen, H.S., Wium-Andersen, T., Hvitved-Jacobsen, T., 2008. Influence of pipe material and surfaces on sulfide related odor and corrosion in sewers. Water Res. 42 (15), 4206–4214. https://doi.org/10.1016/j.watres.2008.07.013.

Noda, I., 2004. Advances in two-dimensional correlation spectroscopy. Vib. Spectrosc. 36 (2), 143–165. https://doi.org/10.1016/j.vibspec.2003.12.016.

Qin, Z., Yao, Y., Zhao, J., Fu, H., Zhang, S., Qiu, L., 2021. Investigation of migration rule of rainwater for sponge city roads under different rainfall intensities. Environ. Geochem. Health 1–13. https://doi.org/10.1007/s10653-021-01104-9.

Ranjan, V.P., Joseph, A., Goel, S., 2021. Microplastics and other harmful substances released from disposable paper cups into hot water. J. Hazard. Mater. 404, 124118. https://doi.org/10.1016/j.jhazmat.2020.124118.

Shi, Y., Liu, P., Wu, X., Shi, H., Huang, H., Wang, H., Gao, S., 2021. Insight into chain scission and release profiles from photodegradation of polycarbonate microplastics. Water Res. 195, 116980. https://doi.org/10.1016/j.watres.2021.116980.

Song, N., Wu, D., Xu, H., Jiang, H., 2022. Integrated evaluation of the reactive oxygen species (ROS) production characteristics in one large lake under alternating flood and drought conditions. Water Res. 225, 119136. https://doi.org/10.1016/j.watres.2022.119136.

Su, Y., Hu, X., Tang, H., Lu, K., Li, H., Liu, S., Ji, R., 2022. Steam disinfection releases micro (nano) plastics from silicone-rubber baby teats as examined by optical photothermal infrared microspectroscopy. Nat. Nanotechnol. 17 (1), 76–85. https://doi.org/10.1038/s41565-021-00998-x.

Suhrhoff, T.J., Scholz-Böttcher, B.M., 2016. Qualitative impact of salinity, UV radiation and turbulence on leaching of organic plastic additives from four common plastics—a lab experiment. Mar. Pollut. Bull. 102 (1), 84–94. https://doi.org/10.1016/j.marpolbul.2015.11.054.

Toapanta, T., Okoffo, E.D., Ede, S., O'Brien, S., Burrows, S.D., Ribeiro, F., Thomas, K.V., 2021. Influence of surface oxidation on the quantification of polypropylene microplastics by pyrolysis gas chromatography mass spectrometry. Sci. Total Environ. 796, 148835. https://doi.org/10.1016/j.scitotenv.2021.148835.

Toensmeier, P., 2020. Plastics and the circular economy: sustainability was the issue at ANTEC®, as conference speakers highlighted techniques to increase recycling and reduce waste. Plast. Eng. 76 (6), 12–15. https://doi.org/10.1002/peng.20326.

Wang, Z., An, C., Chen, X., Lee, K., Zhang, B., Feng, Q., 2021. Disposable masks release microplastics to the aqueous environment with exacerbation by natural weathering. J. Hazard. Mater. 417, 126036. https://doi.org/10.1016/j.jhazmat.2021.126036.

Yang, Y., Chen, J., Chen, Z., Yu, Z., Xue, J., Luan, T., Zhou, S., 2022. Mechanisms of polystyrene microplastic degradation by the microbially driven Fenton reaction. Water Res. 223, 118979. https://doi.org/10.1016/j.watres.2022.118979.

Yin, C.F., Xu, Y., Zhou, N.Y., 2020. Biodegradation of polyethylene mulching films by a co-culture of Acinetobacter sp. strain NyZ450 and Bacillus sp. strain NyZ451 isolated from Tenebrio molitor larvae. Int. Biodeterior. Biodegradation 155, 105089. https://doi.org/10.1016/j.ibiod.2020.105089.

Zhang, Z., Chen, Y., 2020. Effects of microplastics on wastewater and sewage sludge treatment and their removal: a review. Chem. Eng. J. 382, 122955. https://doi.org/10.1016/j.cej.2019.122955.

Zhang, X., Liu, C., Liu, J., Zhang, Z., Gong, Y., Li, H., 2022. Release of microplastics from typical rainwater facilities during aging process. Sci. Total Environ. 813, 152674. https://doi.org/10.1016/j.scitotenv.2021.152674.

Zhu, K., Jia, H., Sun, Y., Dai, Y., Zhang, C., Guo, X., Zhu, L., 2020. Long-term phototransformation of microplastics under simulated sunlight irradiation in aquatic environments: roles of reactive oxygen species. Water Res. 173, 115564. https://doi.org/10.1016/j.watres.2020.115564.